The Journal of Neuroscience, January 1, 2000, 20(1):171–178

α_{1E} Subunits Form the Pore of Three Cerebellar R-Type Calcium Channels with Different Pharmacological and Permeation Properties

Angelita Tottene,[1] Stephen Volsen,[2] and Daniela Pietrobon[1]

[1]Department of Biomedical Sciences, University of Padova, 35121 Padova, Italy, and [2]Lilly Research Center, Eli Lilly Company Limited, Windlesham, Surrey GU20 6PH, United Kingdom

R-type Ca^{2+} channels cooperate with P/Q- and N-type channels to control neurotransmitter release at central synapses. The leading candidate as pore-forming subunit of R-type channels is the α_{1E} subunit. However, R-type Ca^{2+} currents with permeation and/or pharmacological properties different from those of recombinant Ca^{2+} channels containing α_{1E} subunits have been described, and therefore the molecular nature of R-type Ca^{2+} channels remains not completely settled. Here, we show that the R-type Ca^{2+} current of rat cerebellar granule cells consists of two components inhibited with different affinity by the α_{1E} selective antagonist SNX482 (IC_{50} values of 6 and 81 nM) and a third component resistant to SNX482. The SNX482-sensitive R-type current shows the unique permeation properties of recombinant α_{1E} channels; it is larger with Ca^{2+} than with Ba^{2+} as charge carrier, and it is highly sensitive to Ni^{2+} block and has a voltage-dependence of activation consistent with that of G2 channels with unitary conductance of 15 pS. On the other hand, the SNX482-resistant R-type current shows permeation properties similar to those of recombinant α_{1A} and α_{1B} channels; it is larger with Ba^{2+} than with Ca^{2+} as charge carrier, and it has a low sensitivity to Ni^{2+} block and a voltage-dependence of activation consistent with that of G3 channels with unitary conductance of 20 pS. Gene-specific knock-down by antisense oligonucleotides demonstrates that the different cerebellar R-type channels are all encoded by the α_{1E} gene, suggesting the existence of α_{1E} isoforms with different pore properties.

Key words: calcium channel; α_{1E} subunit; antisense oligonucleotides; cerebellum; granule cells; permeation; toxin-resistant calcium current

Most neurons of the CNS display several types of high-voltage activated Ca^{2+} channels, pharmacologically classified as L-, N-, P/Q, and R-type (Dunlap et al., 1995). R-type Ca^{2+} currents were first described by Tsien and coworkers as corresponding to the residual current observed in rat cerebellar granule neurons after pharmacological block of L-, N-, and P/Q-type Ca^{2+} channels (Zhang et al., 1993; Randall and Tsien, 1995). Subsequently, R-type currents with different biophysical properties were described in different types of neurons (Tottene et al., 1996; Hilaire et al., 1997; Magnelli et al., 1998; Wu et al., 1998), and single channel recordings revealed that rat cerebellar granule cells coexpress two Ca^{2+} channels, called G2 and G3, differing in unitary conductance and threshold for activation but both classified as R-type on the basis of their resistance to all specific Ca^{2+} channel inhibitors (Forti et al., 1994; Tottene et al., 1996).

The molecular basis of R-type channels is not completely settled. The leading candidate as pore-forming subunit of R-type channels is the α_{1E} subunit. However, of the two R-type channels of cerebellar granule cells, only G2 has a unitary conductance of 15 pS, similar to that of recombinant α_{1E} channels (Schneider et al., 1994; Wakamori et al., 1994; Bourinet et al., 1996), whereas G3 has a conductance of 20 pS (Forti et al., 1994; Tottene et al., 1996). Whereas recombinant α_{1E} channels have the unique property among high-voltage activated channels of carrying more current with Ca^{2+} than with Ba^{2+} (Bourinet et al., 1996), and in addition are very sensitive to Ni^{2+} block (Soong et al., 1993; Schneider et al., 1994; Williams et al., 1994; Zamponi et al., 1996), native R-type currents show Ba^{2+} over Ca^{2+} current ratios ranging from 0.9 to 2 (Zhang et al., 1993; Hilaire et al., 1997; Magnelli et al., 1998), and some require relatively high concentrations of Ni^{2+} to be blocked (Tottene et al., 1996; Magnelli et al., 1998; Wu et al., 1998). SNX482, the first selective antagonist of recombinant α_{1E} channels, failed to inhibit R-type currents in several types of central neurons, including rat cerebellar granule cells (Newcomb et al., 1998). However, the R-type current of these neurons was reduced by antisense oligonucleotides (ONs) against α_{1E} (Piedras-Renteria and Tsien, 1998).

Whereas splice variants of α_1 subunits with different pharmacological properties are known (Bourinet et al., 1999; Hans et al., 1999), there are to date no reports of splice variants or subunit combinations with different permeation properties and/or single channel conductance. Therefore, it remains unclear whether the different native R-type channels and in particular G2 and G3 are all encoded by the α_{1E} gene. Indeed, it has been suggested that some R-type currents might actually be supported by channels containing α_{1A} or α_{1B} subunits with low affinity for their specific toxins (Nooney et al., 1997; Magnelli et al., 1998).

Using an antisense strategy, here we show that the α_{1E} gene encodes both native SNX482-sensitive R-type channels with the unique permeation properties of recombinant α_{1E} channels and native SNX482-resistant R-type channels showing none of these properties.

Received Aug. 9, 1999; revised Oct. 18, 1999; accepted Oct. 20, 1999.

This work was supported by Telethon-Italy Grant 720 to D.P. A.T. was supported by the Lilly Postdoctoral Research Program. We thank Drs. G. Miljanich and L. Nadasdi of Elan Pharmaceuticals Inc. for providing SNX483, and Carlo Berizzi and Francesca Bolcato for help in performing some of the experiments.

Correspondence should be addressed to Daniela Pietrobon, Department of Biomedical Sciences, University of Padova, V.le G. Colombo 3, 35121 Padova, Italy. E-mail: dani@civ.bio.unipd.it.

MATERIALS AND METHODS

Cell culture. Cerebellar granule cells were grown in primary culture after enzymatic and mechanical dissociation from 6- to 7-d-old Wistar rats according to the procedure of Levi et al. (1984). The cells were plated on poly-L-lysine-coated glass coverslips and kept in Basal Eagle's medium supplemented with 10% fetal calf serum, 25 mM KCl, 2 mM glutamine, and 60 μg/ml gentamycin. Cytosine arabinoside (10 μM) was added to the culture 18 hr after plating to inhibit the proliferation of non-neuronal cells. Granule cells were the large majority of the cells in the cultures and were morphologically identified by their oval or round cell body, small size, and bipolar neurites. Experiments were usually performed on granule cells grown for 5–7 d *in vitro*.

Transfection with oligonucleotides. One day after plating, cerebellar granule cells were transfected using polyethylenimine (PEI) (50 kDa; Sigma, St. Louis, MO) as transfecting agent (Lambert et al., 1996). DNA (1 μg) and 60 nmol of PEI (neutralized to pH 7.0 with HCl) were first separately diluted in 13 μl of 150 mM NaCl. PEI–DNA particles were thereafter obtained by gently mixing the two solutions. Cells, plated in 3.5 cm Petri dishes, were incubated for 1–2 hr in the PEI–DNA solution previously diluted to 0.8 ml with serum-free culture medium. In each culture, part of the cells were exposed to fluorescein-conjugated antisense ONs and part of the cells to fluorescein-conjugated scrambled oligonucleotides (160 nM). ONs were fully phosphorothioated and were designed and produced by Biognostik GmbH (Gottingen, Germany). Specifically, we used antisense ONs against nucleotides 81–98 of the α_{1E} subunit (Soong et al., 1993), corresponding to the N-terminal cytoplasmic region (sequence: GCATATTTCCTGACAATG), against nucleotides 414–431 of the α_{1A} subunit (Starr et al., 1991), corresponding to segment S2 of repeat I (sequence: CCAATGAAATAGGGTTCT), and the corresponding scrambled oligonucleotides (sequences: ACTACTACACTAGACTAC and TCAAAACGAATGCAGTTG, respectively).

Electrophysiology. Whole-cell patch-clamp recordings followed standard techniques (Hamill et al., 1981). Currents were recorded with an Axopatch-200 patch-clamp amplifier (Axon Instruments, Foster City, CA), low-pass filtered at 1 kHz (−3 dB; eight-pole Bessel filter), sampled at 5 kHz using a Digidata 1200 interface and pClamp6 software (Axon Instruments), and stored for later analysis on a computer. Compensation (typically 70–80%) for series resistance was generally used, and only data from cells with a voltage error of <3 mV were analyzed. Experiments were performed at room temperature (21–25°C).

To measure the R-type calcium current in isolation, cells were preincubated for 10 min into a recording chamber containing Tyrode's solution supplemented with 1 μM ω-conotoxin-GVIA (ω-CgTx-GVIA) (Bachem, Budendorf, Switzerland), 3 μM ω-conotoxin-MVIIC (ω-CTx-MVIIC or SNX230 provided by Neurex Corporation, Menlo Park, CA), 5 μM nimodipine (gift from Dr. Hof, Sandoz, Basel, Switzerland), and 0.1 mg/ml cytochrome c (Sigma, St. Louis, MO). After attainment of the whole-cell configuration, cells were perfused with the external recording solution containing: 5 mM $BaCl_2$, 148 mM TEA-Cl, 10 mM HEPES (adjusted to pH 7.4 with TEA-OH), 5 μM nimodipine, and 0.1 mg/ml cytochrome c. Control experiments in which ω-CgTx-GVIA and ω-CTx-MVIIC were sequentially applied at increasing times after perfusion with external solution, established that slow unblocking of the toxins could account for at most 10% of the R-type current measured after 30 min (the maximal duration of our recordings). Internal solution contained (in mM): 100 Cs-methanesulfonate, 5 $MgCl_2$, 30 HEPES, 10 EGTA, 4 ATP, 0.5 GTP, and 1 mM cAMP (adjusted to pH 7.4 with CsOH). The perfusion system consisted of six microcapillary Teflon tubes glued together and placed inside a standard plastic pipette (Gilson Medical Electronics, Villiers-le-Bel, France) at ~12 mm from the tip (~1.2 mm diameter), which was cut to have a flute beak shape, and positioned close to the cell. The tubes were fed by gravity from reservoirs containing external solution with or without toxins. Switching between different solutions was controlled by solenoid valves. Delay time for complete solution change was <8 sec. Cytocrome c (0.1 mg/ml) was included in all recording solutions to block nonspecific peptide binding sites. Liquid junction potential at the pipette tip was −8 mV (pipette negative), and that between the Tyrode's solution in the experimental chamber and the external recording solution (flowing from the capillary tube) was −4 mV; these two junction potentials should be added to all voltages to obtain the correct values of membrane potential in whole-cell recordings (Neher, 1992). Isolated cells were chosen for recording. The experiment was discarded if cells showed signs of inadequate space clamping, such as notch-like current discontinuities, slow components in the decay of capacitative currents (in response to hyperpolarizing pulses), or slow tails not fully inhibited by nimodipine (Forti and Pietrobon, 1993). Barium currents were corrected on-line for leak and capacitative currents with the P/4 pulse protocol. Averages are given as mean ± SEM. The statistical significance of paired values was tested by an ANOVA, followed by a *post hoc t* test.

The neurotoxin SNX482, a 41 amino acid peptide present in the venom of the African tarantula *Histerocrates gigas* (Newcomb et al., 1998) was kindly provided by G. Miljanich and L. Nadasdi (Elan Pharmaceuticals Inc., Menlo Park, CA).

RESULTS

The peptide neurotoxin SNX482 selectively inhibits recombinant calcium channels containing α_{1E} subunits with an IC_{50} for block of ~30 nM (Newcomb et al., 1998). We assessed the sensitivity to SNX482 of the R-type calcium current of rat cerebellar granule cells in primary culture. To isolate the R-type calcium current, L-, N-, and P/Q-type calcium channels were completely inhibited using saturating concentrations of nimodipine, ω-CgTx-GVIA, and ω-Ctx-MVIIC (Hillyard et al., 1992; Zhang et al., 1993; McDonough et al., 1996; Tottene et al., 1996). As shown in Figure 1*A* (*top panel*), 10 nM SNX482 slowly inhibited a fraction of the R-type current. No significant further inhibition was observed with 30 nM toxin, but 100 nM toxin inhibited more, indicating the presence of at least two components of R-type current with different sensitivity to SNX482. The lack of significant further inhibition by 200 nM toxin with respect to 100 nM, shown in the *bottom panel* of Figure 1*A*, indicates that the R-type calcium current of cerebellar granule cells actually comprises three components with different sensitivity to the toxin. The three R-type current components, R_a, R_b, and R_c, can be seen in the dose–response curve in Figure 1*B*. The values of IC_{50} for inhibition of the three components, obtained by fitting the data points with the sum of three Hill equations, were 6, 81, and 654 nM (fractional contributions: 32, 17, and 51%, for R_a, R_b, and R_c, respectively). Figure 1 then shows that the R-type calcium current of rat cerebellar granule cells comprises two components, R_a and R_b, inhibited by concentrations of SNX482 close to those that inhibit recombinant α_{1E} channels, and in addition, a third component, R_c, that can be considered as toxin-resistant because SNX482 is not a selective blocker of α_{1E} channels at the concentrations required to inhibit R_c (Newcomb et al., 1998). The one order of magnitude difference in IC_{50} for inhibition of components R_a and R_b is reminiscent of the difference in affinity for ω-agatoxin IVA (ω-AgaIVA) of P- and Q-type calcium currents (Randall and Tsien, 1995). The two components R_a and R_b differ also in the time course of inhibition by SNX482. As shown by the representative experiment in Figure 4*A*, the kinetics of inhibition by 30 nM toxin (component R_a) were faster (τ of 50 ± 5 sec; $n = 10$) than those of inhibition by 200 nM toxin, sequentially added after 30 nM (component R_b: τ of 74 ± 8 sec; $n = 11$).

Recombinant calcium channels containing α_{1E} subunits are characterized by a high sensitivity to Ni^{2+} block (Soong et al., 1993; Schneider et al., 1994; Williams et al., 1994; Zamponi et al., 1996) and by a larger macroscopic current with Ca^{2+} as charge carrier compared with Ba^{2+} (Bourinet et al., 1996; and our unpublished observations with both human $\alpha_{1E\text{-}d}$ and $\alpha_{1E\text{-}3}$ subunits). Both observations point to distinct permeation properties of α_{1E} with respect to α_{1A}, α_{1B}, and α_{1C} channels. Tottene et al. (1996) have shown previously that only 50% of the R-type current of cerebellar granule cells shows a high sensitivity to Ni^{2+} block, requiring concentrations of 30–50 μM Ni^{2+} to be fully inhibited. The less sensitive component was inhibited with an IC_{50} of 153 μM. Figure 2 shows that the R-type current remaining in the

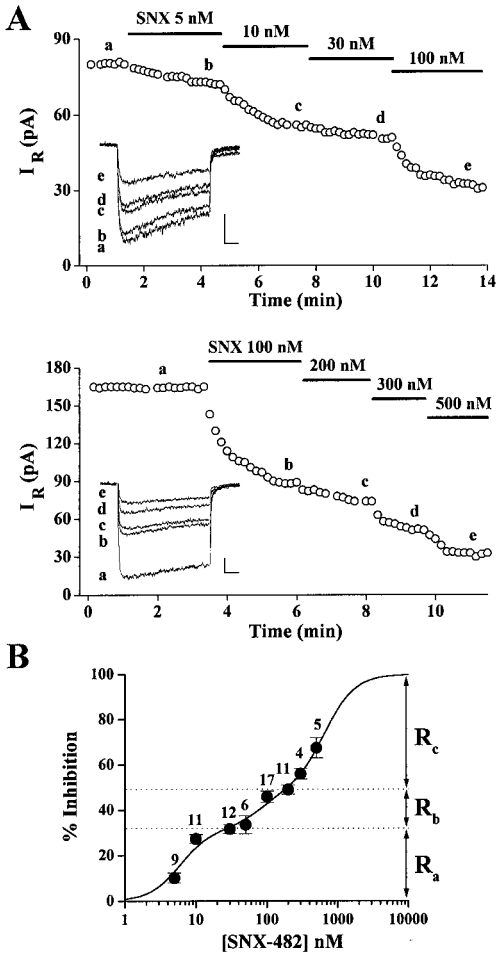

Figure 1. Three components of R-type current with different sensitivity to SNX482 in rat cerebellar granule cells: R_a, R_b, and R_c. Whole-cell recordings of R-type current with 5 mM Ba^{2+} as charge carrier after inhibition of L-, N-, and P/Q-type currents with saturating concentrations of nimodipine, ω-CgTx-GVIA, and ω-CTx-MVIIC (see Materials and Methods). Test depolarizations to −10 mV were delivered every 10 sec from holding potential V_h of −90 mV. *A*, Plots of peak R-type Ba^{2+} current, I_R, versus time for two representative experiments in which either 5, 10, 30, and 100 nM SNX482 (*top panel*; cell U89D) or 100, 200, 300, and 500 nM SNX482 (*bottom panel*; cell U126A) were sequentially applied. Representative average current traces ($n = 4$) taken at times indicated by *a*, *b*, *c*, *d*, and *e* are shown in the *insets*. Calibration: 25 pA, 20 msec. *B*, Dose–response curve for SNX482 inhibition of the R-type current, obtained by averaging the fractional inhibitions produced by successive applications of at least three concentrations of toxin in 21 cells. The number of cells from which the average inhibition at any given concentration was obtained is indicated above the *symbols*. The *continuous line* is the sum of three Hill equations with $n_a = n_b = n_c = 2$ and K_a of 36 nM (IC_{50a} of 6 nM), K_b of 6.6 μM (IC_{50b} of 81 nM), and K_c of 428 μM (IC_{50c} of 654 nM). A Hill coefficient larger than one was necessary to adequately fit the data points (the fit further improved with $n = 3$). Failure to completely reach steady-state at low toxin concentrations cannot completely account for the requirement of Hill coefficients greater than one, because, from fitting the time course of inhibition with a single exponential, a maximal 25% underestimation of the inhibition at the lowest toxin concentration can be calculated. A Hill coefficient larger than one ($n = 1.4$) was also necessary to best fit the dose–response curve for SNX482 inhibition of recombinant calcium channels containing human $\alpha_{1E\text{-}d}$ subunits (our unpublished observations).

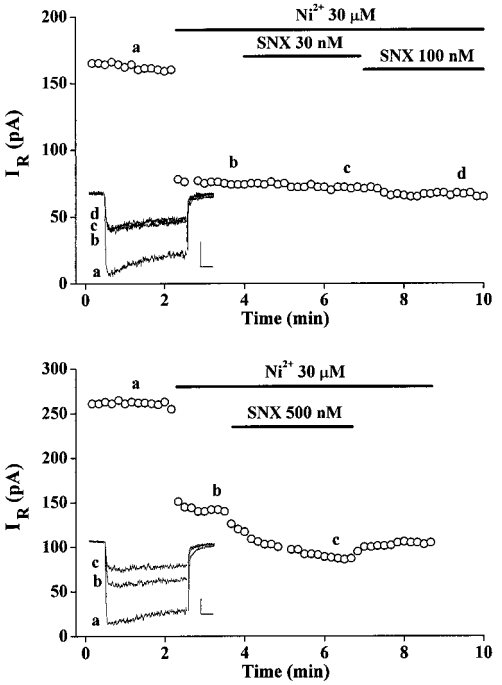

Figure 2. The R_c current is less sensitive to Ni^{2+} block than R_a and R_b currents. Whole-cell recordings of R-type current as in Figure 1. Plots of peak R-type Ba^{2+} current versus time for two representative experiments in which 30 μM Ni^{2+} was applied, and then either 30 and 100 nM SNX482 were sequentially applied (*top panel*; cell U213C) or 500 nM SNX482 was applied (*bottom panel*; cell U137A) in the continuous presence of Ni^{2+}. Representative current traces taken at times indicated by *a*, *b*, *c*, and *d* are shown in the *insets*. Calibration: 50 pA, 20 msec. The lack of inhibition by 30 and 100 nM SNX482 means that both components R_a and R_b are fully inhibited by 30 μM Ni^{2+}. The partial inhibition by 500 nM SNX482 means that component R_c is not inhibited by 30 μM Ni^{2+}.

presence of 30 μM Ni^{2+} was not further inhibited by concentrations of SNX482 (30 and 100 nM) that completely blocked components R_a and R_b; however, it was partially inhibited by 500 nM SNX482, a concentration that partially inhibited component R_c. These occlusion experiments show that the two R-type current components with relatively high affinity for SNX482 are both very sensitive to Ni^{2+} block, whereas the R-type calcium channels resistant to the toxin have a relatively low sensitivity to Ni^{2+} block.

Figure 3 further shows that R_c, the R-type current component resistant to SNX482, has different permeation properties than the two SNX482-sensitive components. Whereas the total R-type current at the peak of the current–voltage (*I–V*) relationship had similar amplitude with Ba^{2+} or Ca^{2+} as charge carrier (Fig. 3*A*), the R_c current remaining in the presence of 200 nM SNX482 was larger with Ba^{2+} (Fig. 3*B*). On average, the ratio I_{Ca2+}/I_{Ba2+} was 0.99 ± 0.02 ($n = 4$) and 0.72 ± 0.09 ($n = 3$) for total R-type and R_c currents, respectively (significantly different at $p < 0.02$). One can then argue that the two SNX482-sensitive current components (R_a and R_b) are larger with Ca^{2+} than with Ba^{2+} as charge carrier and therefore have permeation properties similar to those of recombinant α_{1E} channels (compare also their high sensitivity to Ni^{2+} block). On the other hand, the R_c component has permeation properties similar to those of α_{1A}, α_{1B}, and α_{1C} channels.

Tottene et al. (1996) have shown previously that at least two different calcium channels, G2 and G3, contribute to the R-type calcium current of cerebellar granule cells. The two channels

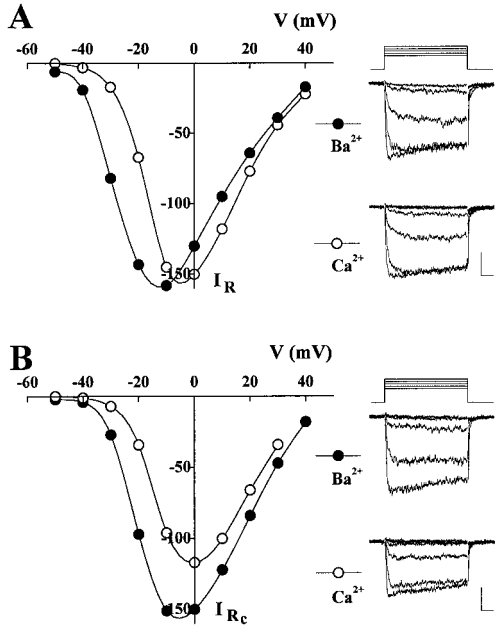

Figure 3. The total R-type current has similar amplitude with Ca^{2+} and Ba^{2+} as charge carrier, whereas the R_c current is larger with Ba^{2+}. Whole-cell recordings with either 5 mM Ba^{2+} or 5 mM Ca^{2+} as charge carrier. Perfusion of the cells with the Ba^{2+} solution was followed by perfusion with the Ca^{2+} solution and then again with the Ba^{2+} solution. Increasing test depolarizations from −50 to + 40 mV were delivered every 5 sec from V_h of −90 mV in each solution. *A*, Current–voltage relationships of R-type current, I_R, and representative traces at increasing depolarizations with either 5 mM Ca^{2+} (○; V of −50 to 0 mV) or 5 mM Ba^{2+} (●; perfused after Ca^{2+}; V of −50 to −10 mV). Calibration: 50 pA, 20 msec. Cell U81A. *B*, Current–voltage relationships of R-type current in the presence of 200 nM SNX482, I_{Rc}, and representative traces at increasing depolarizations with either 5 mM Ca^{2+} (○; V of −50 to 0 mV) or 5 mM Ba^{2+} (●; perfused after Ca^{2+}; V of −50 to −10 mV). Calibration: 50 pA, 20 msec. Cell U214D.

differ mainly in single channel current and conductance and in voltage range for activation (Forti et al., 1994). G2 channels, with unitary conductance of 15 pS, activate at ~15 mV more negative voltages than G3 channels with unitary conductance of 20 pS. It appears reasonable to predict that G2 channels with unitary conductance similar to that of recombinant α_{1E} channels should support the two SNX-sensitive current components R_a and R_b (with permeation properties similar to those of recombinant α_{1E} channels) and that G3 channels with different unitary conductance should support the SNX-resistant R_c component (with permeation properties different from those of recombinant α_{1E} channels). If this hypothesis is correct, component R_c should activate at more positive voltages than components R_a and R_b. To verify this hypothesis and eventually obtain information on the relative sensitivity to SNX482 of G2 and G3 channels, we performed whole-cell recordings in which 30 and 200 nM SNX482 were sequentially added, and the *I–V* relationship was measured before and after each toxin addition. According to the dose–response curve in Figure 1, 30 nM toxin completely inhibits component R_a, which is then given by the difference between the R-type current measured in the presence and absence of 30 nM toxin; 200 nM toxin should completely inhibit component R_b, which can then be obtained as the difference between the R-type current measured in the presence of 200 and 30 nM toxin. Component R_c is given by the current remaining in the presence of 200 nM toxin.

As shown by the representative experiment in Figure 4*A*, the *I–V* curve in the presence of 30 nM toxin was shifted toward more positive voltages with respect to that in its absence, and the *I–V* curve in the presence of 200 nM toxin was shifted in the same direction with respect to that in the presence of 30 nM toxin. Figure 4*B* shows the average normalized *I–V* curves for the three components; component R_a activates at slightly more negative voltages than R_b, and both R_a and R_b activate at more negative voltages than R_c. The three R-type components had slightly different kinetics of inactivation (5 ± 2, 24 ± 3, and 17 ± 2% decay in 136 msec for R_a, R_b, and R_c, respectively; $n = 10$) (see Fig. 4*A*). The different current–voltage relationships, the different kinetics of inactivation, and the different time course of inhibition together support the notion that different calcium channels underlie the R-type current components identified on the basis of the dose–response curve for SNX482. The data are consistent with the conclusion that the channels with the highest affinity for SNX482 correspond to G2, the R channel subtypes activating at more negative voltages. Given the large difference in half-voltage for activation (18 mV) between G2 and G3, the R-type channels resistant to SNX482 most likely correspond to G3, the R channel subtypes with unitary conductance different from that reported for α_{1E} channels. Figure 4*C* shows that the steady-state inactivation curve of the current remaining in the presence of 200 nM SNX482 was almost identical to that of the total R-type current. Steady-state inactivation of the calcium channels that underlie the three R-type current components then occurred at quite negative voltages ($V_{1/2}$ of −76 mV) in a similar voltage range. Steady-state inactivation of both G2 and G3 channels occurred in a similar negative voltage range.

Both the pharmacological and permeation properties of the R-type channels resistant to SNX482 of rat cerebellar granule cells are quite different from those of recombinant channels containing α_{1E} subunits. α_{1B}, α_{1A}, or α_{1E} subunits with low affinity for their specific toxins or an unknown α_1 subunit appear equally likely as the pore-forming subunits of these channels. To investigate the molecular basis of the SNX482-resistant R-type channels and to directly show that α_{1E} subunits are the pore-forming subunits of the SNX482-sensitive R-type channels, we turned to an antisense strategy.

Cerebellar granule cells were transfected with fluorescein-conjugated anti-α_{1E} antisense ON 1 d after plating. R-type calcium current densities were measured at 3, 4, and 5 d after transfection. At each day, control R-type current densities were measured in cells from the same culture transfected with fluorescein-conjugated scrambled ON. Transfected neurons were identified by their fluorescent nuclei. As shown in Figure 5*A*, α_{1E} subunit knock-down strongly decreased the R-type current of cerebellar granule cells. A maximum decrease of 87% was achieved 4 d after transfection (from 23 ± 4 to 3 ± 1 pA/pF; $p \ll 0.001$). After 3 d, the current was already 75% reduced ($p < 0.001$), suggesting a turnover time of ~3 d for these α_1 subunits. Figure 5*B* shows that α_{1E} subunit knock-down decreased to a similar extent both the fraction of R-type current inhibited by 30 μM Ni^{2+} (corresponding to components R_a and R_b) and the fraction of R-type current remaining not inhibited (corresponding to component R_c). Analysis of the development of the different components of control R-type current with increasing days in culture shows that the small increase in total R-type current observed between days 3 and 4 after transfection (corresponding to the fourth and fifth day in culture) is caused by an increased expression of the SNX482-resistant R-type channels with low

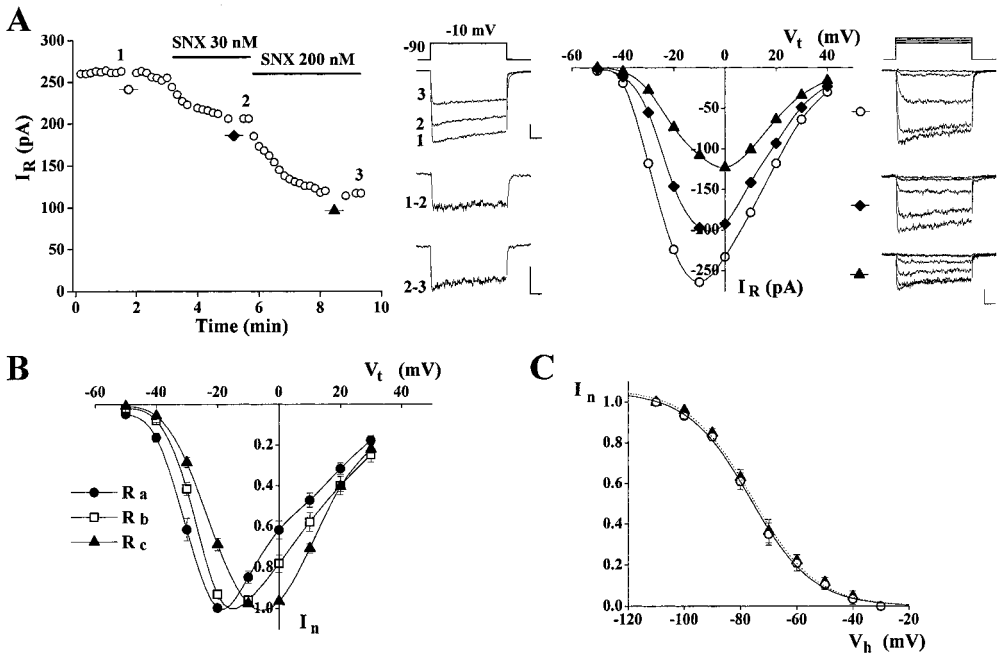

Figure 4. Different voltage-dependence of activation and similar voltage-dependence of inactivation of the three R-type current components. Whole-cell recordings of R-type current with 5 mM Ba^{2+} as charge carrier. *A*, *Left panel*, Plot of peak R-type Ba^{2+} current, I_R, versus time for an experiment in which 30 and 200 nM SNX482 were sequentially applied. Test depolarizations to −10 mV were delivered every 10 sec from V_h of −90 mV. Representative average current traces ($n = 4$) taken at times indicated by *1*, *2*, and *3*, together with difference trace *1–2*, corresponding to the R_a current component, and difference trace *2–3*, corresponding to the R_b current component, are shown in the *middle inset*. Calibration: 50 pA, 20 msec. *Right panel*, *I–V* relationships measured at times indicated by *symbols* in the absence (○) and presence of 30 nM (♦) and 200 nM (▲) SNX482. Representative traces at increasing test depolarizations (V_t of −50 to −10 mV) are shown in the *right inset*. Calibration: 50 pA, 20 msec. Cell U198E. *B*, Average peak normalized current, I_n, as a function of test voltage, V_t, for the three components R_a (●; $n = 12$), R_b (□; $n = 13$), and R_c (▲; $n = 13$). For each cell, the current was normalized with respect to maximal peak current. At each voltage, R_a is obtained as difference between the R-type currents measured in the presence and absence of 30 nM toxin; R_b is obtained as difference between the R-type currents measured in the presence of 200 and 30 nM toxin, and R_c is the R-type current remaining in the presence of 200 nM toxin. *C*, Average peak normalized R-type current, I_n, at −10 mV as a function of holding potential, V_h, in the absence (total R, ○; $n = 8$) and presence of 200 nM SNX482 (R_c, ▲; $n = 6$). For each cell, the current was normalized with respect to the peak current at V_h of −110 mV. The data points were best fit by a Boltzmann distribution function of the form $I_n = I_{n\,max} \times (1 + \exp((V - V_{1/2})/k))^{-1}$ with $V_{1/2}$ of −76 mV and k of 11 mV for both total R and R_c currents.

affinity for Ni^{2+}. The R-type current remaining in the presence of 30 μM Ni^{2+} increased 78% ($p < 0.04$) between days 3 and 4 after transfection, whereas the R-type current inhibited by the same concentration of Ni^{2+} did not change.

The specificity of the anti-α_{1E} antisense ON was tested by investigating its effect on the N-type calcium current. Figure 6*A* shows that the current density inhibited by 1 μM ω-CgTx-GVIA was similar in cells transfected with antisense and scrambled ON, whereas in the same cells the R-type current was 73% decreased in antisense-transfected cells. As an additional test, we ascertained that an anti-α_{1A} antisense oligonucleotide, which proved to be effective in decreasing the P-type current in Purkinje cells (Gillard et al., 1997), did not affect the R-type current of cerebellar granule cells. Figure 6*B* shows that the R-type current was similar in cells transfected with anti-α_{1A} antisense and scrambled ON.

Thus, quite unexpectedly, the antisense data show that α_{1E} subunits form the pore of the R subtypes of calcium channels of rat cerebellar granule cells with pharmacological and permeation properties different from those of recombinant channels containing α_{1E} subunits. Moreover, they directly show that the two SNX482-sensitive R subtypes both contain α_{1E} subunits as pore-forming subunits.

DISCUSSION

Using an antisense strategy combined with electrophysiology and the new selective pharmacological tool provided by SNX482, we show that rat cerebellar granule cells coexpress calcium channels containing α_{1E} subunits with widely different pharmacological and biophysical (including permeation) properties.

Previous work on recombinant calcium channels containing α_{1E} subunits has led to the identification of a few specific properties distinguishing them from high-voltage activated α_{1A}, α_{1B}, and α_{1C} channels. The specific properties, common to all the different isoforms of α_{1E} studied so far, include the following (1) a high sensitivity to Ni^{2+} block (Soong et al., 1993; Schneider et al., 1994; Williams et al., 1994); (2) the peptide neurotoxin SNX482 as the only selective, high-affinity antagonist (Newcomb et al., 1998, and our unpublished observations), (3) a larger macroscopic current with Ca^{2+} than with Ba^{2+} as charge carrier (Bourinet et al., 1996; and our unpublished observations with both human $\alpha_{1E\text{-}d}$ and $\alpha_{1E\text{-}3}$ subunits), and (4) a single channel conductance of 12–15 pS (Schneider et al., 1994; Wakamori et al., 1994; Bourinet et al., 1996).

Here, we show that these properties are shared by the native calcium channels containing α_{1E} subunits, which account for the two SNX482-sensitive components of the R-type current of rat cerebellar granule cells. The one order of magnitude difference in IC_{50} for inhibition of these two components (6 and 81 nM) is reminiscent of the difference in affinity for ω-AgaIVA of P- and Q-type calcium currents (Randall and Tsien, 1995). It has been shown that α_{1A} subunits are the pore-forming subunits of both P- and Q-type channels (Gillard et al., 1997; Piedras-Renteria and Tsien, 1998) and that alternative splicing of the α_{1A} gene may give rise to calcium channels with pharmacological and biophysical properties similar to those of P- and Q-type channels (Bourinet et al., 1999). Likewise, alternative splicing of the α_{1E} gene may possibly account for the different sensitivity to SNX482 of the two R-type current components. Alternatively, the different pharmacology may be attributable to different combinations with auxiliary subunits (Moreno et al., 1997).

Single channel recordings have shown previously that two calcium channels, G2 and G3, with different unitary conductance and voltage-dependence of activation, contribute to the R-type

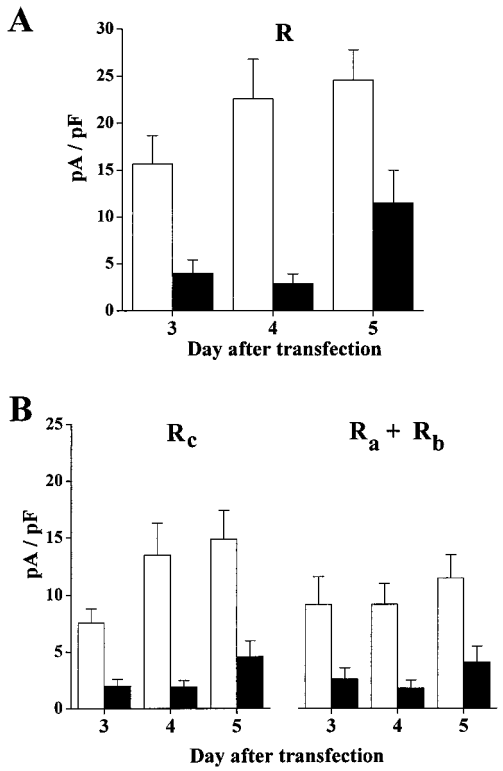

Figure 5. α_{1E} subunit knock-down by specific antisense oligonucleotides decreases to a similar extent the three R-type current components of rat cerebellar granule cells. Whole-cell recordings of R-type current as in Figure 1. Data are pooled from four neuronal cultures. In each culture, current densities were measured in both antisense ON- and scrambled ON-transfected cells at 3, 4, and 5 d after transfection. *A*, Total R-type current densities as a function of time after transfection, measured in cerebellar granule cells transfected with α_{1E} antisense ON (*black bars*) and with scrambled ON (*white bars*). Peak R-type current densities were measured 3 min after entering into the whole-cell configuration. Antisense ON: $n = 13$, 15, and 8 at days 3, 4, and 5, respectively. Scrambled ON: $n = 12$, 11, and 11 at days 3, 4, and 5, respectively. The reduction of the R-type current in antisense-transfected cells was significant at each day in culture (75%, $p < 0.001$; 87%, $p \ll 0.001$; and 53%, $p < 0.02$ at day 3, 4, and 5, respectively). *B*, R-type current densities as a function of time after transfection, measured in the presence of 30 μM Ni^{2+} (corresponding to component R_c; *left panel*) and inhibited by 30 μM Ni^{2+} (corresponding to components R_a and R_b; *right panel*) in cerebellar granule cells transfected with α_{1E} antisense ON (*black bars*) and with scrambled ON (*white bars*). Ni^{2+} was applied 3 min after entering into the whole-cell configuration. Antisense ON: $n = 11$, 11, and 5 at days 3, 4, and 5, respectively. Scrambled ON: $n = 10$, 6, and 8 at days 3, 4, and 5, respectively. The reduction of the different R-type current components in the antisense-transfected neurons was significant at each day in culture (R_c: 74%, $p < 0.001$; 86%, $p \ll 0.001$; 69%, $p < 0.02$; R_a and R_b: 72%, $p < 0.02$; 80%, $p < 0.001$; 64%, $p < 0.02$ at 3, 4, and 5 d, respectively).

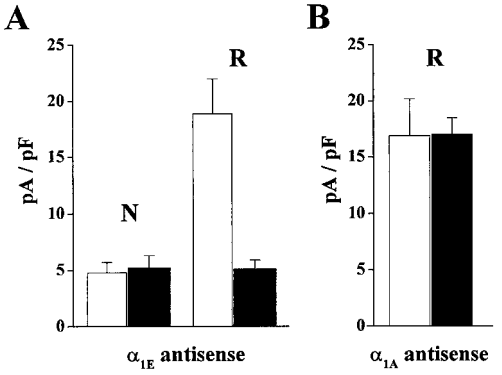

Figure 6. The N-type current is not affected by α_{1E} antisense ONs, and the R-type current is not affected by α_{1A} antisense ONs. Whole-cell recordings with 5 mM Ba^{2+} as charge carrier. Voltage protocol as in Figure 1. *A*, (N + R)-type Ba^{2+} current densities were measured 4 d after transfection in cerebellar granule cells transfected with α_{1E} antisense ON (*black bars*) and with scrambled ON (*white bars*) in the continuous presence of 5 μM nimodipine after incubation of the neurons with 3 μM ω-CTx-MVIIC to irreversibly block P/Q-type channels; ω-CgTx-GVIA (1 μM) was then applied. N-type and R-type current densities were obtained from the current densities inhibited by ω-CgTx-GVIA and remaining in the presence of ω-CgTx-GVIA, respectively. N-type current densities were similar in antisense ON- ($n = 7$) and scrambled ON- ($n = 8$) transfected cells, whereas R-type currents were 73% smaller in antisense ON-transfected cells ($p < 0.002$). *B*, R-type current densities measured 4–5 d after transfection in cerebellar granule cells transfected with α_{1A} antisense ON (*black bars*; $n = 10$) and with scrambled ON (*white bars*; $n = 9$) were similar.

calcium current of rat cerebellar granule cells (Forti et al., 1994; Tottene et al., 1996). G2 channels have unitary conductance and current (15 pS, 0.6 pA at 0 mV) similar to those of recombinant α_{1E} channels, whereas G3 channels have larger unitary conductance and current (20 pS, 0.8 pA at 0 mV). G2 channels activate at ~15 mV more negative voltages than G3. A comparable difference in voltage range of activation has been found here between the component of R-type current most sensitive to SNX482 and that resistant to SNX482, the first activating at more negative voltages than the latter. Our data are consistent with the conclusion that the R-type channels with high affinity for SNX482 correspond to G2, and those with very low affinity for SNX482 correspond to G3. Given the small difference in voltage-dependence of activation of the two SNX482-sensitive components of R-type current, it appears likely that, at the single channel level, the channels underlying these two components were lumped together under the name of G2. This conclusion is further supported by the fact that, in cell-attached patches, G2 channels were observed more frequently than G3 channels (Forti et al., 1994), and R-type channels different from G2 and G3 were extremely rare (our unpublished observations).

The component of the R-type calcium current of rat cerebellar granule cells resistant to SNX482 shows none of the "specific" properties of recombinant α_{1E} channels; it is not very sensitive to Ni^{2+} block, it is larger with Ba^{2+} than with Ca^{2+} as charge carrier, and, most likely, it is supported by G3 channels with conductance of 20 pS. Nonetheless, strikingly, this component is suppressed after transfection of the neurons with a specific anti-α_{1E} antisense oligonucleotide. Therefore, in addition to calcium channels containing α_{1E} subunits with permeation properties considered as typical of α_{1E} subunits, rat cerebellar granule cells express calcium channels containing α_{1E} subunits with permeation properties more typical of α_{1A}, α_{1B}, or α_{1C} subunits. It is highly unlikely that these permeation properties are caused by a particular combination with auxiliary subunits, because β and α_2-δ subunits do not appear to affect single channel conductance and permeation of recombinant α_1 channels (Wakamori et al., 1993, 1999; and our unpublished observations). Most likely, these peculiar native R-type channels contain a novel α_{1E} variant, whose properties have not been studied in heterologous expression systems.

The component of R-type current resistant to SNX482, accounting for ~50% of the R-type current of our cerebellar granule cells, has many properties in common with the original R-type current described in the same neurons by Zhang et al.

(1993). The common properties include the ratio I_{Ca}/I_{Ba} lower than 1, the relatively low sensitivity to Ni^{2+} block, the resistance to SNX482 (Newcomb et al., 1998), and the reduction by specific anti-α_{1E} antisense oligonucleotides (Piedras-Renteria and Tsien, 1998). However, in cerebellar granule cells cultured under the conditions of Zhang et al. (1993), there was no evidence for the presence of additional components of R-type current inhibited with high affinity by SNX482 (Newcomb et al., 1998). The most likely explanation is the expression of different α_{1E} splice variants in neurons cultured under different conditions and obtained from rats of different age. Similarly, expression of different α_{1A} splice variants (and/or different β subunits) may explain the P-type pharmacology found by Tottene et al. (1996) in contrast with the Q-type pharmacology found by Randall and Tsien (1995) in the same neurons (Moreno et al., 1997; Bourinet et al., 1999).

Reverse transcription-PCR analysis of the mRNA isolated from our primary cultures of cerebellar granule cells has shown the expression of up to six different α_{1E} isoforms alternatively spliced in the II–III loop and the C terminus, some of which had not been cloned before (Schramm et al., 1999). There is evidence for different relative expression of these isoforms in different brain regions and during development (Pereverzev et al., 1998; Schramm et al., 1999). Two of the isoforms do not show differences in biophysical properties (Pereverzev et al., 1998). The functional properties of the other four isoforms remain unknown. Splice variants of α_{1A}, α_{1B}, and α_{1C} with different kinetics and/or voltage-dependence of the macroscopic calcium current have been described previously (Lin et al., 1997; Soldatov et al., 1997; Bourinet et al., 1999; Hans et al., 1999). However, splice variants of calcium channel α_1 subunits with different permeation properties and different unitary conductance have never before been reported.

Labeling with antibodies of brain slices has shown localization of α_{1E} subunits in both cell bodies and dendrites of many types of neurons (Volsen et al., 1995; Yokoyama et al., 1995) and more recently also in calyx-type synaptic terminals of the brainstem (Wu et al., 1999). Wu et al. (1998) have shown that R-type channels contribute to action potential-evoked transmitter release at these synapses. Most likely, R-type channels participate in controlling evoked release in many other central synapses (Turner et al., 1993), including cerebellar parallel fiber synapses (Mintz et al., 1995). The localization in cell bodies and dendrites suggest additional postsynaptic roles of R-type channels, e.g., G2-type channels with a relatively low threshold of activation might have a role in synaptic integration and the generation of calcium spikes (D'Angelo et al., 1997). It is reasonable to hypothesize that R-type channels with different voltage-dependence of activation and different unitary conductance as those coexpressed in cerebellar granule cells may have a specialized function in different neuronal processes. Alternative splicing of α_{1E} subunits may allow different subcellular localizations, different modulation, and different binding to specific membrane proteins of the different R-type channels. Indeed, in the case of α_{1A} subunits, it has been shown that the II–III loop and the C-terminal region, the two regions alternatively spliced in the α_{1E} isoforms expressed in cerebellar granule cells, are involved in binding important proteins, such as syntaxin (Rettig et al., 1996) and calmodulin (Lee et al., 1999), respectively, and that alternatively spliced II–III loop isoforms have a different ability to bind syntaxin (Rettig et al., 1996) and have a different subcellular distribution (Sakurai et al., 1996).

REFERENCES

Bourinet E, Zamponi GW, Stea A, Soong TW, Lewis BA, Jones LP, T YD, Snutch TP (1996) The α_{1E} calcium channel exhibits permeation properties similar to low-voltage-activated calcium channels. J Neurosci 16:4983–4993.

Bourinet E, Soong TW, Sutton K, Slaymaker S, Mathews E, Monteil A, Zamponi GW, Nargeot J, Snutch TP (1999) Splicing of α_{1A} subunit gene generates phenotypic variants of P- and Q-type calcium channels. Nature Neuroscience 2:407–415.

D'Angelo E, De Filippi G, Rossi P, Taglietti V (1997) Synaptic activation of Ca^{2+} action potentials in immature rat cerebellar granule cells *in situ*. J Neurophysiol 78:1631–1642.

Dunlap K, Luebke JI, Turner TJ (1995) Exocytotic Ca^{2+} channels in mammalian central neurons. Trends Neurosci 18:89–98.

Forti L, Pietrobon D (1993) Functional diversity of L-type calcium channels in rat cerebellar neurons. Neuron 10:437–450.

Forti L, Tottene A, Moretti A, Pietrobon D (1994) Three novel types of voltage-dependent calcium channels in rat cerebellar neurons. J Neurosci 14:5243–5256.

Gillard SE, Volsen SG, Smith W, Beattie RE, Bleakman D, Lodge D (1997) Identification of pore-forming subunit of P-type calcium channels: an antisense study on rat cerebellar Purkinje cells in culture. Neuropharmacology 36:405–409.

Hamill O, Marty A, Neher E, Sakmann B, Sigworth F (1981) Improved patch-clamp techniques for high-resolution current recording from cells and cell-free membrane patches. Pflügers Arch 391:85–100.

Hans M, Urrutia A, Deal C, Brust PF, Stauderman K, Ellis SB, Harpold MM, Johnston EC, Williams ME (1999) Structural elements in domain IV that influence biophysical and pharmacological properties of human α_{1A}-containing high-voltage-activated calcium channels. Biophys J 76:1384–1400.

Hilaire C, Diochot S, Desmadryl G, Richard S, Valmier J (1997) Toxin-resistant calcium currents in embryonic mouse sensory neurons. Neuroscience 80:267–276.

Hillyard DR, Monje VD, Mintz IM, Bean BP, Nadasdi L, Ramachandran J, Miljanich G, Azimi-Zoonooz A, McIntosh JM, Cruz LJ, Imperial JS, Oliveira BM (1992) A new Conus peptide ligand for mammalian presynaptic Ca^{2+} channels. Neuron 9:69–77.

Lambert RC, Maulet Y, Dupont JL, Mykita S, Craig P, Volsen S, Feltz A (1996) Polyethylenimine-mediated DNA transfection of peripheral and central neurons in primary culture: probing Ca^{2+} channel structure and function with antisense oligonucleotides. Mol Cell Neurosci 7:239–246.

Lee A, Wong ST, Gallagher D, Li B, Storm DR, Scheuer T, Catterall WA (1999) Ca^{2+}/calmodulin binds to and modulates P/Q-type calcium channels. Nature 399:155–159.

Levi G, Aloisi M, Ciotti M, Gallo V (1984) Autoradiographic localization and depolarization-induced release of amino acids in differentiating granule cells cultures. Brain Res 290:77–86.

Lin Z, Haus S, Edgerton J, Lipscombe D (1997) Identification of functionally distinct isoforms of the N-type Ca^{2+} channel in rat sympathetic ganglia and brain. Neuron 18:153–166.

Magnelli V, Baldelli P, Carbone E (1998) Antagonists-resistant calcium currents in rat embryo motoneurons. Eur J Neurosci 10:1810–1825.

McDonough SI, Swartz KJ, Mintz IM, Boland LM, Bean BP (1996) Inhibition of calcium channels in rat central and peripheral neurons by ω-conotoxin MVIIC. J Neurosci 16:2612–2623.

Mintz IM, Sabatini BL, Regehr WG (1995) Calcium control of transmitter release at a cerebellar synapse. Neuron 15:675–688.

Moreno H, Rudy B, Llinas R (1997) β subunits influence the biophysical and pharmacological differences between P- and Q-type calcium currents expressed in a mammalian cell line. Proc Natl Acad Sci USA 94:14042–14047.

Neher E (1992) Correction for liquid junction potentials in patch clamp experiments. Methods Enzymol 207:123–131.

Newcomb R, Szoke B, Palma A, Wang G, Chen X, Hopkins W, Cong R, Miller J, Urge L, Tarczy-Hornoch K, Loo JA, Dooley DJ, Nadasdi L, Tsien RW, Lemos J, Miljanich G (1998) Selective peptide antagonist of the class E calcium channel from the venom of the tarantula *Hysterocrates gigas*. Biochemistry 37:15353–15362.

Nooney JM, Lambert RC, Feltz A (1997) Identifying neuronal non-L Ca^{2+} channels—more than stamp collecting? Trends Pharmacol Sci 18:363–371.

Pereverzev A, Klockner U, Henry M, Grabsch H, Vajna R, Olyschlager S, Viatchenko-Karpinski S, Schroder R, Hescheler J, Schneider T (1998) Structural diversity of the voltage-dependent Ca^{2+} channel α_{1E}-subunit. Eur J Neurosci 10:916–925.

Piedras-Renteria ES, Tsien RW (1998) Antisense oligonucleotides against α_{1E} reduce R-type calcium currents in cerebellar granule cells. Proc Natl Acad Sci USA 95:7760–7765.

Randall A, Tsien RW (1995) Pharmacological dissection of multiple types of Ca^{2+} channel currents in rat cerebellar granule neurons. J Neurosci 15:2995–3012.

Rettig J, Sheng ZH, Kim DK, Hodson CD, Snutch TP, Catterall WA (1996) Isoform-specific interaction of the α_{1A} subunits of brain Ca^{2+} channels with the presynaptic proteins syntaxin and SNAP-25. Proc Natl Acad Sci USA 93:7363–7368.

Sakurai T, Westenbroek RE, Rettig J, Hell J, Catterall WA (1996) Biochemical properties and subcellular distribution of the BI and rbA isoforms of α_{1A} subunits of brain calcium channels. J Cell Biol 134:511–528.

Schneider T, Wei X, Olcese R, Costantin JL, Neely A, Palade P, Perez-Reyes E, Qin N, Zhou J, Crawford GD, Smith RG, Appel SH, Stefani E, Birnbaumer L (1994) Molecular analysis and functional expression of the human type E neuronal Ca^{2+} channel α_1 subunit. Receptors Channels 2:255–270.

Schramm M, Vajna R, Preverzev A, Tottene A, Klockner U, Pietrobon D, Hescheler J, Schneider T (1999) Isoforms of α_{1E} voltage-gated calcium channels in rat cerebellar granule cells: detection of major calcium channel α_1 transcripts by reverse transcription-polymerase chain reaction. Neuroscience 92:565–575.

Soldatov NM, Zuhlke RD, Bouron A, Reuter H (1997) Molecular structures involved in L-type calcium channel inactivation. J Biol Chem 272:3560–3566.

Soong TW, Stea A, Hodson CD, Dubel SF, Vincent SR, Snutch TP (1993) Structure and functional expression of a member of the low voltage-activated calcium channel family. Science 260:1133–1136.

Starr TVB, Prystay W, Snutch TP (1991) Primary structure of a calcium channel that is highly expressed in the rat cerebellum. Proc Natl Acad Sci USA 88:5621–5625.

Tottene A, Moretti A, Pietrobon D (1996) Functional diversity of P-type and R-type calcium channels in rat cerebellar neurons. J Neurosci 16:6353–6363.

Turner TJ, Adams ME, Dunlap K (1993) Multiple Ca^{2+} channel types coexist to regulate synaptosomal neurotransmitter release. Proc Natl Acad Sci USA 90:9518–9522.

Volsen SG, Day NC, McCormack AL, Smith W, Craig PJ, Beattie R, Ince PG, Shaw PJ, Ellis SB, Gillespie A, Harpold MM, Lodge D (1995) The expression of neuronal voltage-dependent calcium channels in human cerebellum. Mol Brain Res 34:271–282.

Wakamori M, Mikala G, Schwartz A, Yatani A (1993) Single-channel analysis of a cloned human heart L-type Ca^{2+} channel α_1 subunit and the effects of a cardiac β subunit. Biochem Biophys Res Commun 196:1170–1176.

Wakamori M, Niidome T, Furutama D, Furuichi T, Mikoshiba K, Fujita Y, Tanaka I, Katayama K, Yatani A, Schwartz A, Mori Y (1994) Distinctive functional properties of the neuronal BII (class E) calcium channel. Receptors Channels 2:303–314.

Wakamori M, Mikala G, Mori Y (1999) Auxiliary subunits operate as a molecular switch in determining gating behaviour of the unitary N-type Ca^{2+} channel current in *Xenopus* oocytes. J Physiol (Lond) 517.3:659–672.

Williams ME, Marubio LM, Deal CR, Hans M, Brust PF, Philipson LH, Miller RJ, Johnson EC, Harpold MM, Ellis SB (1994) Structure and functional characterization of neuronal α_{1E} calcium channel subtypes. J Biol Chem 269:22347–22357.

Wu LG, Borst JGG, Sakmann B (1998) R-type Ca^{2+} currents evoke transmitter release at a rat central synapse. Proc Natl Acad Sci USA 95:4720–4725.

Wu LG, Westenbroek RE, Borst JGG, Catterall WA, Sakmann B (1999) Calcium channel types with distinct presynaptic localization couple differentially to transmitter release in single calyx-type synapses. J Neurosci 19:726–736.

Yokoyama CT, Westenbroek RE, Hell JW, Soong TW, Snutch TP, Catterall WA (1995) Biochemical properties and subcellular distribution of the neuronal class E calcium channel α_1 subunit. J Neurosci 15:6419–6432.

Zamponi GW, Bourinet E, Snutch TP (1996) Nickel block of a family of neuronal calcium channels: subtype- and subunit-dependent action at multiple sites. J Membrane Biol 151:77–90.

Zhang JF, Randall AD, Ellinor PT, Horne WA, Sather WA, Tanabe T, Schwarz TL, Tsien RW (1993) Distinctive pharmacology and kinetics of cloned neuronal Ca^{2+} channels and their possible counterparts in mammalian CNS neurons. Neuropharmacology 32:1075–1088.